Numerical simulation of the stalled flow within a vaned centrifugal pump

K M Guleren and **A Pinarbasi***
Mechanical Engineering Department, Cumhuriyet University, Sivas, Turkey

Abstract: The main goal of the present work is to analyse the numerical simulation of a centrifugal pump by solving Navier–Stokes equations, coupled with the 'standard k–ε' turbulence model. The pump consists of an impeller having five curved blades with nine diffuser vanes. The shaft rotates at 890 r/min. Flow characteristics are assumed to be stalled in the appropriate region of flowrate levels of 1.31–2.86 l/s. Numerical analysis techniques are performed on a commercial FLUENT package program assuming steady, incompressible flow conditions with decreasing flowrate. Under stall conditions the flow in the diffuser passage alternates between outward jetting when the low-pass-filtered pressure is high to a reverse flow when the filtered pressure is low. Being below design conditions, there is a consistent high-speed leakage flow in the gap between the impeller and the diffuser from the exit side of the diffuser to the beginning of the volute. Separation of this leakage flow from the diffuser vane causes the onset of stall. As the flowrate decreases both the magnitude of the leakage within the vaneless part of the pump and reverse flow within a stalled diffuser passage increase. As this occurs, the stall-cell size extends from one to two diffuser passages. Comparisons are made with experimental data and show good agreement.

Keywords: numerical simulation, vaned centrifugal pump, stalled flow

NOTATION

D	impeller inlet diameter (m)
l	chord length (m)
N	rotational speed (r/min)
N_s	design specific speed
P	static pressure (kPa)
ΔP	static pressure difference between the inlet and outlet (kPa)
Q	flowrate (l/s)
R	radius (m)
t	volute thickness (m)
Z	number of blades
β	blade angle (deg)
ϕ	flowrate constant
φ	angle (deg)

Subscripts

d	diffuser
da	just after diffuser
dPS	diffuser pressure side
dSS	diffuser suction side
i	impeller
ia	just after impeller
1	inlet
2	exit
*	design condition

The MS was received on 16 September 2003 and was accepted after revision for publication on 15 January 2004.
* *Corresponding author: Mechanical Engineering Department, Cumhuriyet University, Sivas 58140, Turkey.*

1 INTRODUCTION

Although there have been serious studies on the stalled flow of pumps and compressors, the mechanical basis of this flow has not been well understood. For the first time, Emmons *et al.* [**1**] gave a logical explanation for stalled flow with the help of cascade theory. More recently, Yoshida *et al.* [**2**] investigated the rotating flow instability in a seven-bladed centrifugal impeller with various diffuser vanes. As well as various stall conditions, it was observed in this study that rotating stall in the diffuser vanes propagated at less than the impeller speed and rotating flow became more obvious when the gap between the impeller and diffuser was increased. Ogata and Ichiro [**3**] made flow measurements comprising the velocity flow field and pressure fluctuations in a

vaned diffuser of a centrifugal compressor. They emphasized that rotating stall occurred at a lower flow condition. Another experimental study into the control of rotating flow in an eight-bladed impeller rotating at 2000 r/min with a vaneless diffuser was made by Tsurusaki and Kinoshita [**4**], who concluded that rotating stalls arose from jets and could be prevented by increasing the flowrate. In addition to these studies, Parrondo *et al*. [**5**] analysed the fluctuating pressure field in the volute of a seven-backward-curved-bladed centrifugal pump in order to characterize the effects of blade–tongue interaction. They concluded that the leading role is played by the tongue in the impeller–volute interaction and there is a strong increase in the magnitude of the dynamic forces in off-design conditions. Sinha *et al*. [**6**] used particle image velocimetry (PIV) and made use of pressure fluctuation measurements to investigate the onset and development of rotating stall within a centrifugal pump having a vaned diffuser. They found that the flow in a stalled diffuser passage, and the occurrence of stall, do not vary significantly with blade orientation. In addition, with decreasing flowrate the magnitudes of leakage and reverse flow within a stalled diffuser passage increase, and the stall-cell size extends from one to two diffuser passages.

Numerical simulation of a centrifugal pump is not easy due to the usual computational fluid dynamics (CFD) difficulties of turbulence modelling, flow separation, boundary layer, etc. In addition, there are also some problems, such as a great number of cells within good skewness due to complex pump geometry, and some difficulties including the equations of the moving zone, where unstructured grids usually give better convergence and good skewness than structured ones. There are also specific problems at the interaction between the impeller and volute, especially around the tongue. Despite this, CFD has proved to be a very useful tool in the analysis of the flow inside pumps, both in design and performance prediction. Much research has been carried out in the last couple of years. Gonzales *et al*. [**7**] produced a numerical simulation to capture the dynamic and unsteady flow effects inside a centrifugal pump due to impeller–volute interaction. They noted that secondary flow patterns are analysed through the helicity magnitude, showing that the stronger effects of secondary flow are concentrated in radial positions close to the impeller exit. They also emphasized that the blade tongue interaction clearly increases the amplitude of fluctuations for off-design conditions. Shi and Tsukamoto [**8**] made a numerical study for the prediction of pressure fluctuations caused by impeller–diffuser interaction in a vaned centrifugal pump and concluded that impeller–diffuser interaction is caused chiefly by potential interaction and wake impingement with the diffuser vanes. Moreover, the 'jet-wake' flow structure at impeller discharge affects the wake–diffuser interaction, but is relatively small compared with stronger viscous wake interactions in the pump. Other numerical analyses of the flow instabilities in the vaned diffuser were carried out by Sano *et al*. [**9**]. This study focused on determining the effects of diffuser performance and of the impeller–diffuser clearance using the commercial software of SCRYU/tetra.

In spite of these experimental and numerical studies, there is limited knowledge or understanding of rotating stall and no detailed numerical study of this flow phenomenon exists. This paper investigates numerically the flow effects due to dynamic interaction between the flow leaving the impeller and the volute tongue within the stalled flow regime of the centrifugal pump. A commercial software package (FLUENT) was used to carry out flow predictions.

2 THE MODEL DESCRIPTION AND COMPUTATIONAL METHOD

The centrifugal pump surface model was generated by the help of SOLIDWORKS and GAMBIT commercial software. The pump has five backward curved blades and nine diffuser vanes. It is important to note that the pump analysed in this paper was not sourced commercially. On the contrary, it was designed for particle image velocity (PIV) analysis and therefore has a constant volute thickness. The detailed pump dimensions are shown in Table 1. The full three-dimensional model can be seen in Fig. 1.

In the present study, a commercial software package (FLUENT) is used for the calculation, with the transport equations being solved using a finite volume

Table 1 Main characteristics of the tested pump

Rotor/impeller	
D_{i1}/D_{i2}	8.51/20.32 cm
Z_i	5 backward-curved
β_{i2}	21.3°
Diffuser/stator	
Z_d	9
D_{d1}/D_{d2}	24.45/30.5 cm
β_{d1}/β_{d2}	10.6°/10.97°
l	13.44 cm
D_{dSS}	14.15 cm
D_{dPS}	24.79 cm
t	1.27 cm
Experimental conditions	
N	890 r/min
Q^*	5.67 l/s
ϕ^*	0.118
N_s	0.49
Flowrate range	2.52–3.78 l/s
Flowrate coefficient range	0.052–0.078



Fig. 1 Full three-dimensional pump model

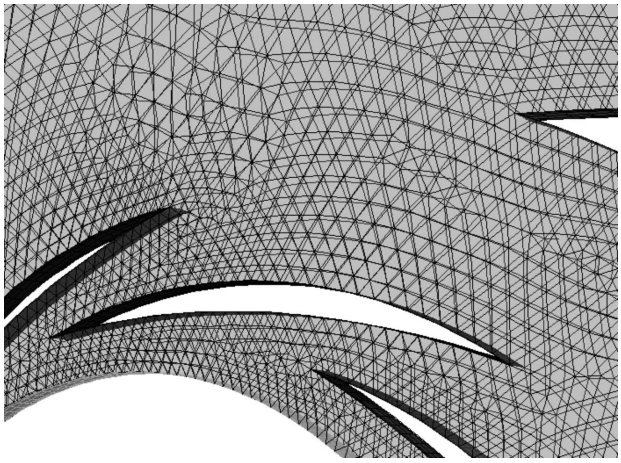


Fig. 3 Three-dimensional zoomed grid model between the tongue and diffuser vanes

method. Unstructured hexahedral cells are generated to define the inlet and outlet zones (37 824 cells and 14 184 cells respectively), while tetrahedral cells are used to define the impeller and volute (45 420 cells and 112 118 cells respectively). In total, the model has 209 546 cells and 153 634 nodes. This size is not enough for a precise boundary layer simulation but it gives correct values for the pump performance and allows details of the main phenomena involved to be analysed. Generally, in a pump it is calculated that the skewness factor of the grid should exceed 0.80. As the model generated is assumed to have a skewness factor generally in the order of 0.85, there is no problem with the grid quality. In addition to this, the only skewness that exceeds 0.7 consists of only 0.24 per cent of the cells. A mid-plane view of the volute of the generated grid can be seen in Fig. 2, while details of the grid between the tongue and diffuser vanes and the impeller grid are shown in Figs 3 and 4 respectively.

The code solves the Reynolds averaged Navier–Stokes equation in a primitive variable form. The effects of turbulence were modelled using the standard k–ε turbulence model. The modelled boundary conditions selected are considered to have more physical meaning for turbomachinery flow simulations, i.e. constant static pressure at the outlet and a variable flowrate proportional to the kinetic energy at the inlet to the impeller. The flowrate is changed by modifying kinetic energy at the inlet condition, which simulates different closing

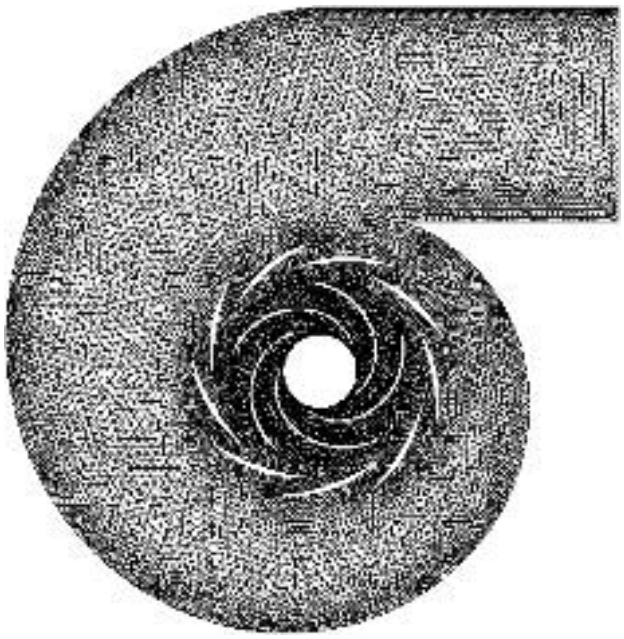


Fig. 2 General grid model at the mid-plane of the pump

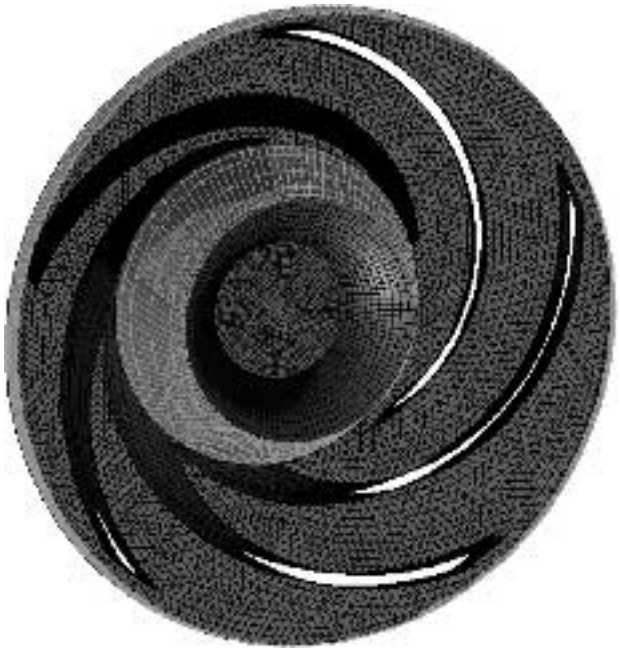


Fig. 4 Three-dimensional grid model for the impeller

positions of the valve. Also, non-slip boundary conditions have been imposed over the impeller blades and diffuser vanes, the volute casing and the inlet pipe wall.

3 NUMERICAL SOLUTION CONTROL

In this study the performance curve of the pump is obtained first. The analysis was performed for more than 15 mass flowrate levels. When the flowrate increases the analysis converges significantly, but the lower flowrate level displays more unstable results due to stalled region effects (the lower flowrate convergence level is around 1.93–4.55 per cent, while the higher flowrate level convergence is closer to 0.72 per cent). This means that in the rotating stall region, the flow does not converge as smoothly when compared to the higher flowrates due to unstable flow phenomena effects. However, within the stalled region, the analysis ran for two or even three days, with a Pentium III-1000 MHz. The outlet pressure fluctuates after approximately 100–150 iterations. After two or three days, the iteration number reaches 2000–2500. As an estimation of pressure gain in the stalled regime, the average pressure values are assumed at the iteration range 100 to 2000–2500.

4 RESULTS AND DISCUSSIONS

4.1 General comments

As a reality check, the performance curve is predicted for various flowrates. The numerical performance curve is then compared with the experimental ones obtained by Sinha *et al*. [**6**]. It is seen that as the flowrate decreases the agreement improves (Fig. 5).

The computational results deal with velocities, pressures and turbulent kinetic energies. In Fig. 6 these parameters are shown for design (3.80 l/s) and stalled flowrate (2.23 l/s) levels while Fig. 7 shows only the stalled (2.23 l/s) flowrate. At design mass flow, the inlet radial velocity to the diffuser is relatively uniform compared with the off-design condition and exit radial absolute velocity distributions indicate that the boundary layers symmetrically developed on both walls; this is in agreement with Sinha's [**6**] experimental observation. At off-design conditions, the distortion of the velocity is exaggerated from the inlet to the exit. This indicates an axial mass migration from the diffuser exit to the impeller at lower mass flow. The exit velocity distributions show that the thicker boundary layer on the suction side of the passage has merged with the thinner boundary layer on the pressure side. The jet exists at higher mass flows with no reverse flow being observed at the exit. The large reverse flow distributions show that the lower flowrate force the flow to turn back into the

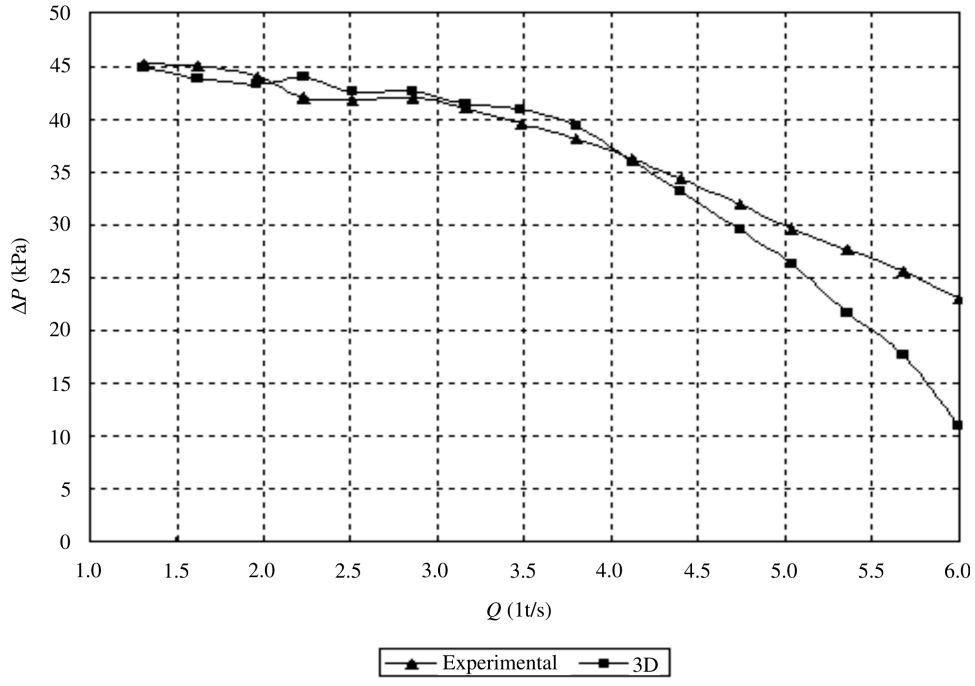


Fig. 5 Pump performance curves, both experimental and numerical

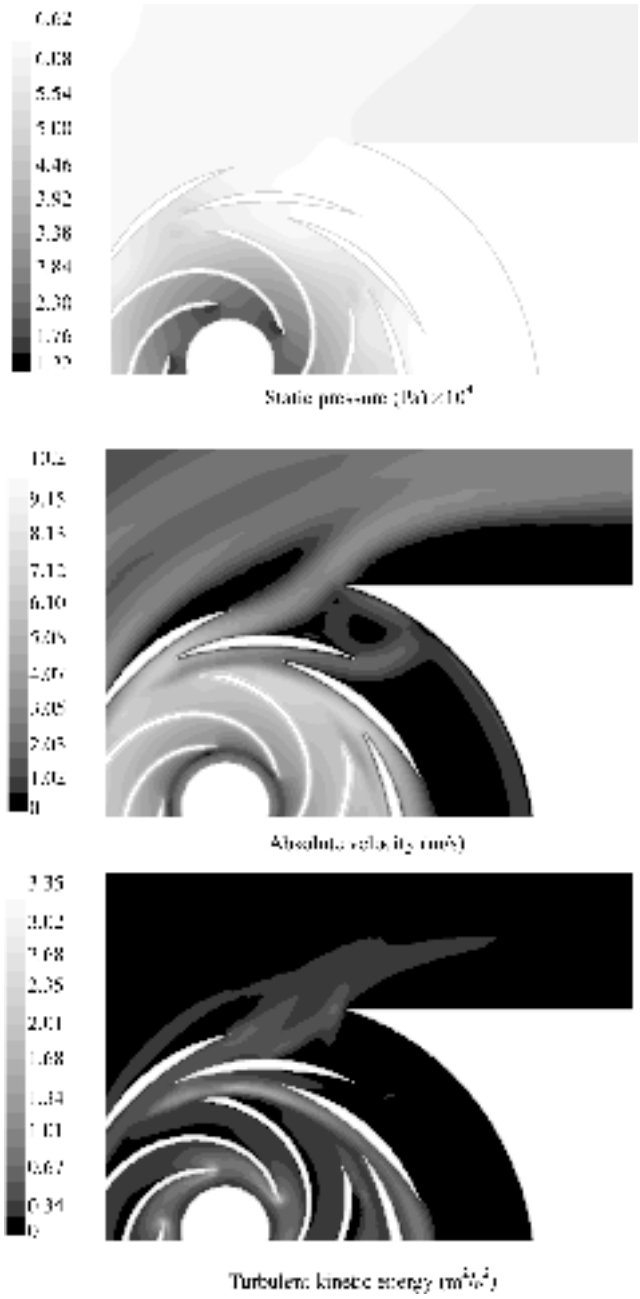


Fig. 6 Flow characteristics at design (3.80 l/s) and stalled (2.23 l/s) flowrates

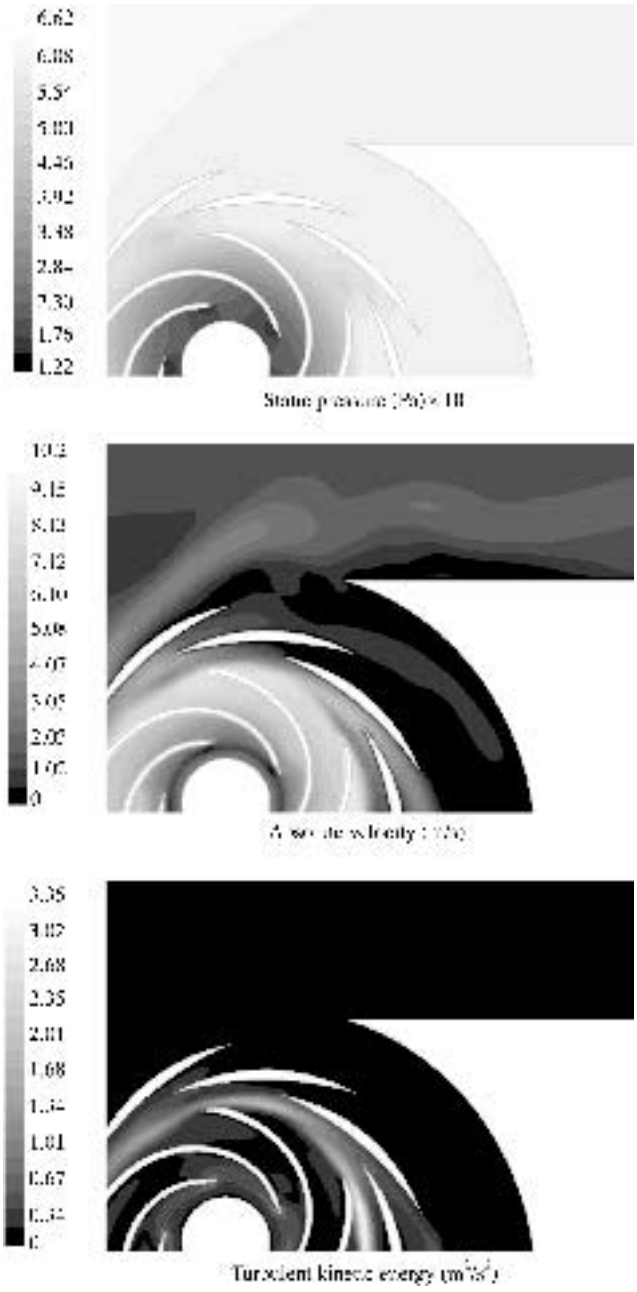


Fig. 7 Flow characteristics at the stalled (2.23 l/s) flowrate

passage, with it separating near the trailing edge of the lower diffuser vane.

A common feature of the static pressure distribution at both flowrate levels is that the contour aligns in a circumferential position and becomes more radial in direction. The curvature of the tongue produces a negative slope as the flow approaches the exit. As the mass flow decreases, the jet nearly disappears. The turbulent kinetic energy magnitudes are higher within the impeller and diffuser gap. This is traced especially at a higher level of flowrate from turbulent kinetic energy contours in Figs 6 and 7, displaying design and stalled flowrate levels respectively. The blade trace is also affected by the flowrate level which accumulates inside the gap like a strip. The losses in the vaneless part of the pump and tongue cause the pump efficiency to reduce.

5 DETAILED COMMENTS

5.1 Diffuser flows

The flow characteristics at lower flowrate levels have been examined computationally to analyse stalled flow

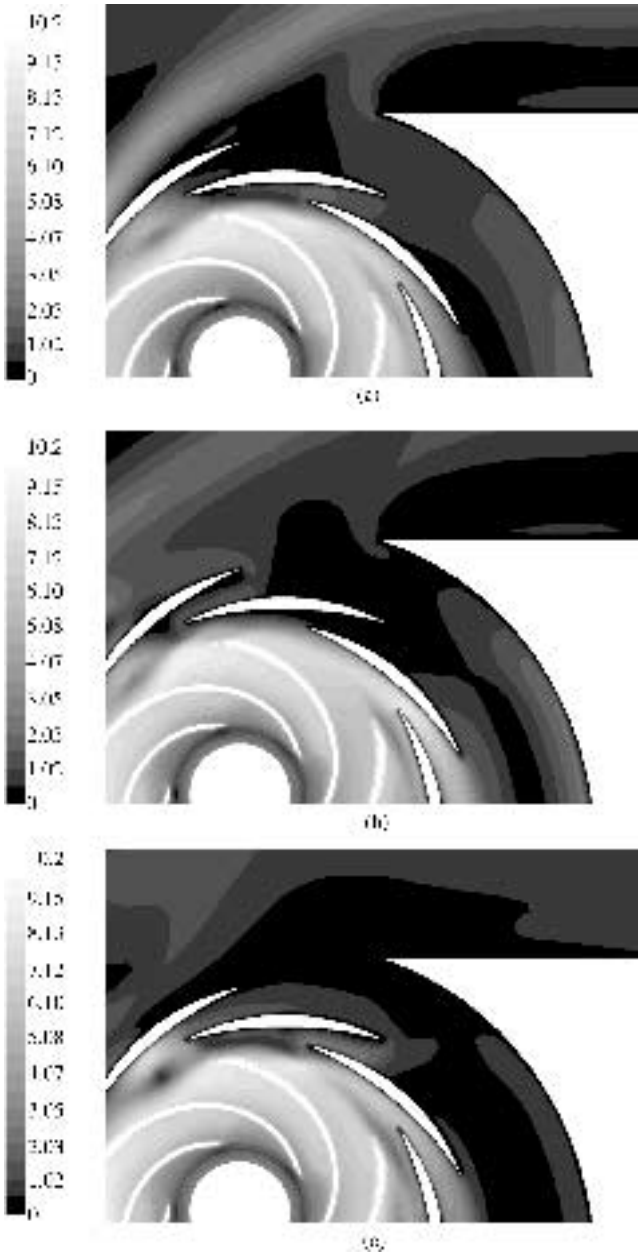


Fig. 8 Flow contours of three flowrates at stall conditions: (a) 2.86 l/s, (b) 1.96 l/s, (c) 1.31 l/s

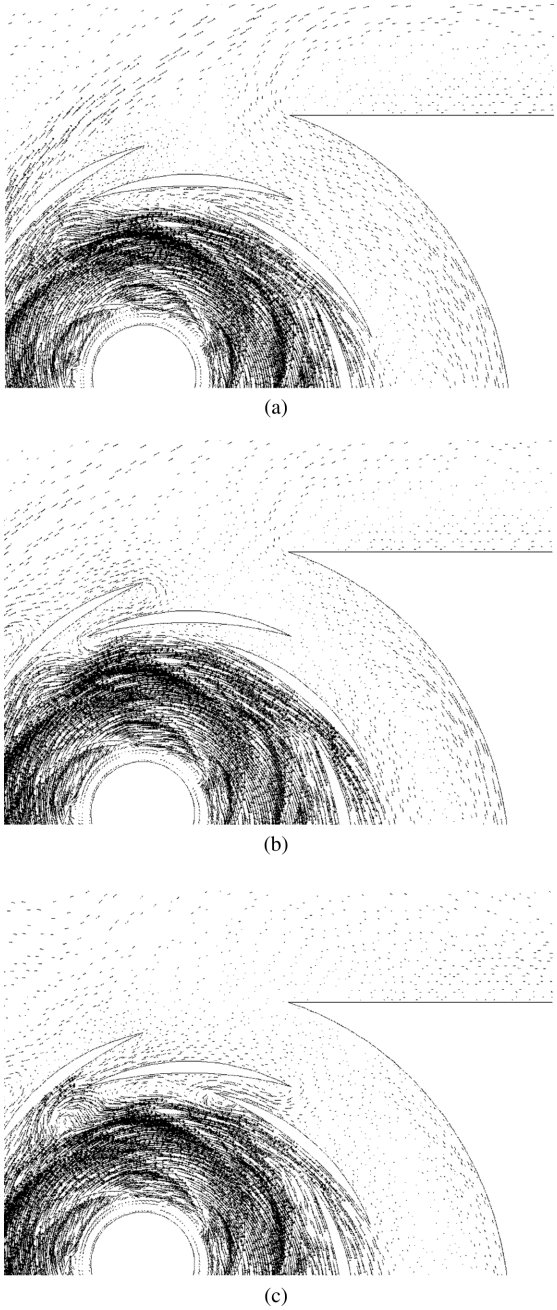


Fig. 9 Flow velocity vectors of three flowrates at stall conditions: (a) 2.86 l/s, (b) 1.96 l/s, (c) 1.31 l/s

at the pump. Figure 8 shows flow contours at three different flowrate levels of 2.86, 1.96 and 1.31 l/s (where the pump stall begins at 2.12 l/s). In all cases the flow is well below design conditions. The different inflow patterns result in different flow structures near the tongue, even though the variation of the diffuser inlet patterns is influenced by the tongue itself. Near the tongue region, each diffuser passage displays a reverse flow from the diffuser discharge back to its throat. This is clearly discernable from velocity vectors around stalled conditions (Fig. 9). The higher pressure region extends to the diffuser inlet, similar to the asymmetric stall. This observation is also supported by Sano *et al.* [**9**].

5.2 Impeller flows

Figures 10 and 11 show the flow characteristics near the shroud and hub wall of the pump respectively. Little difference is observed apart from a small effect on the turbulent kinetic energies. Therefore the mid-plane adequately represents the flow mechanism. Secondary flow and losses appear again on both walls.

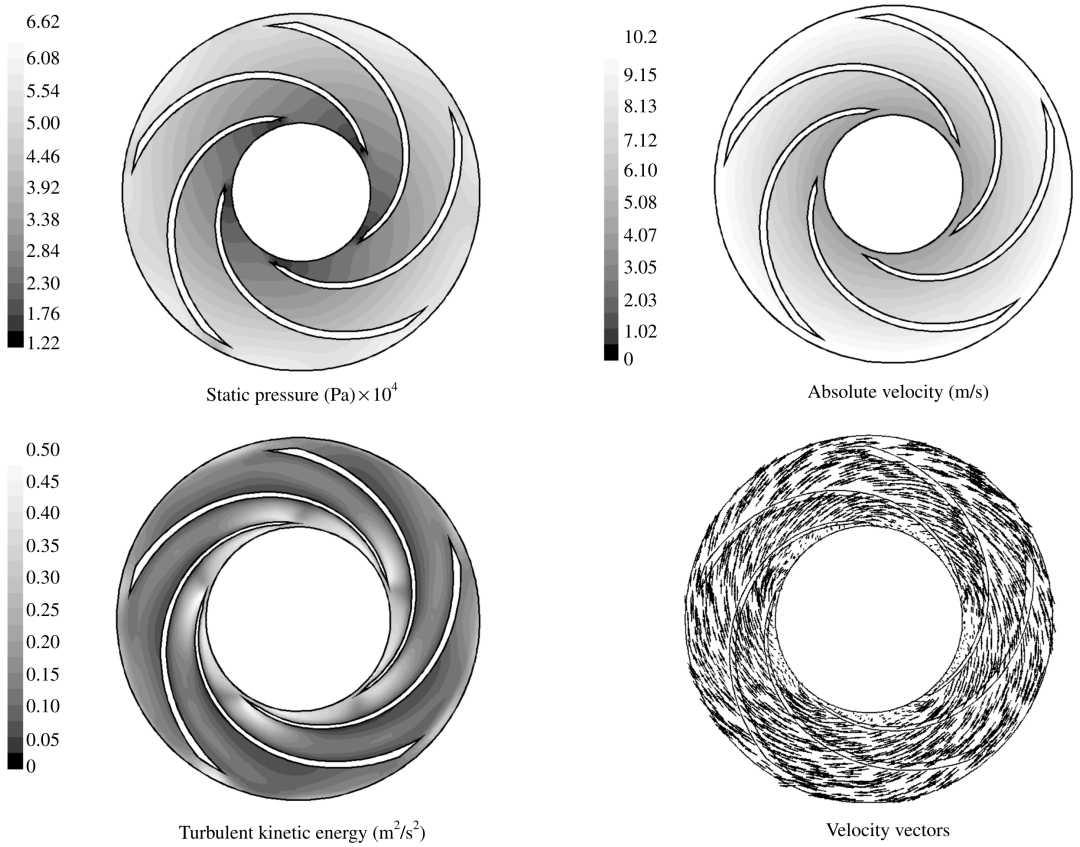


Fig. 10 Flow characteristics on the shroud side at the design flowrate

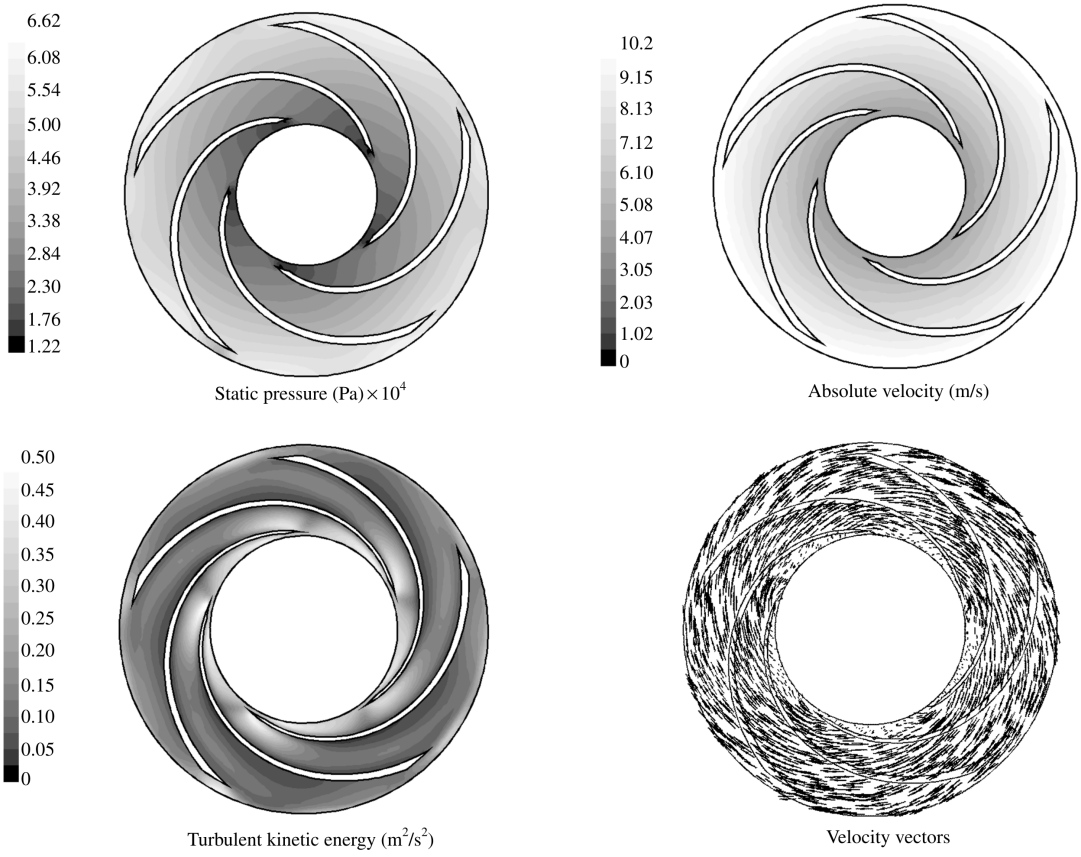


Fig. 11 Flow characteristics on the hub side at the design flowrate

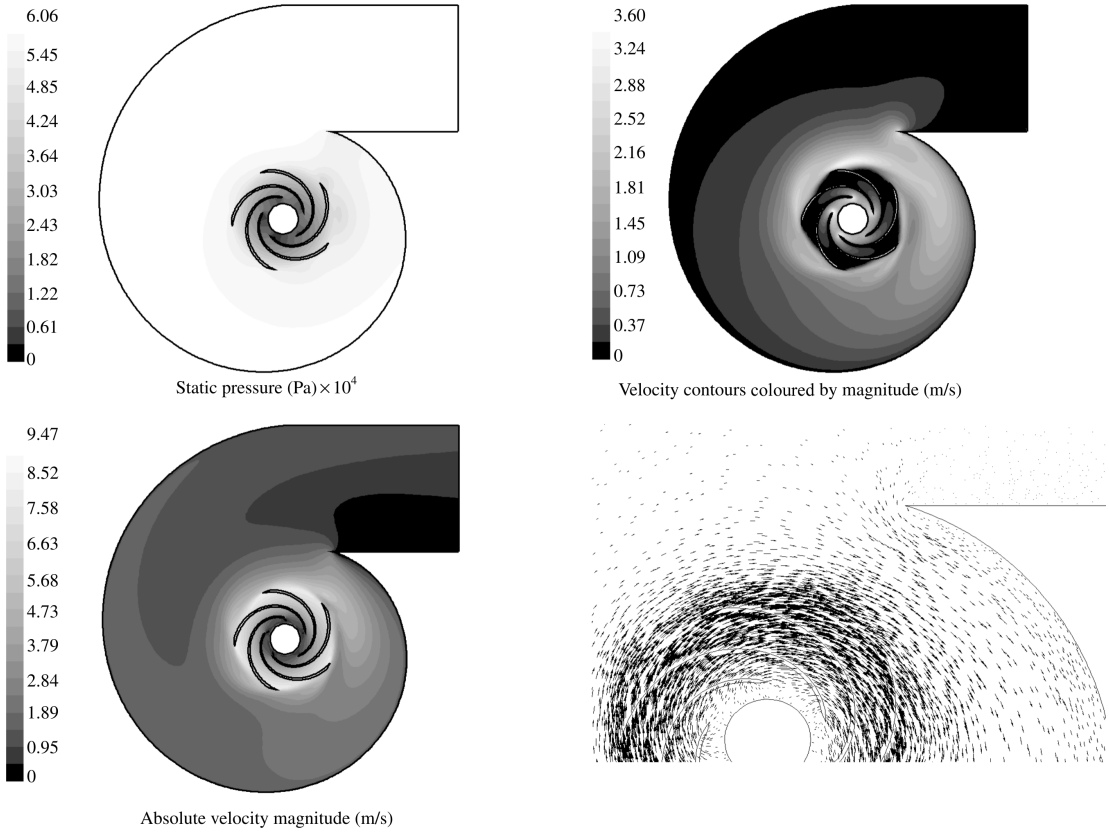


Fig. 12 Flow characteristics without the diffuser at the 1.31 l/s flowrate

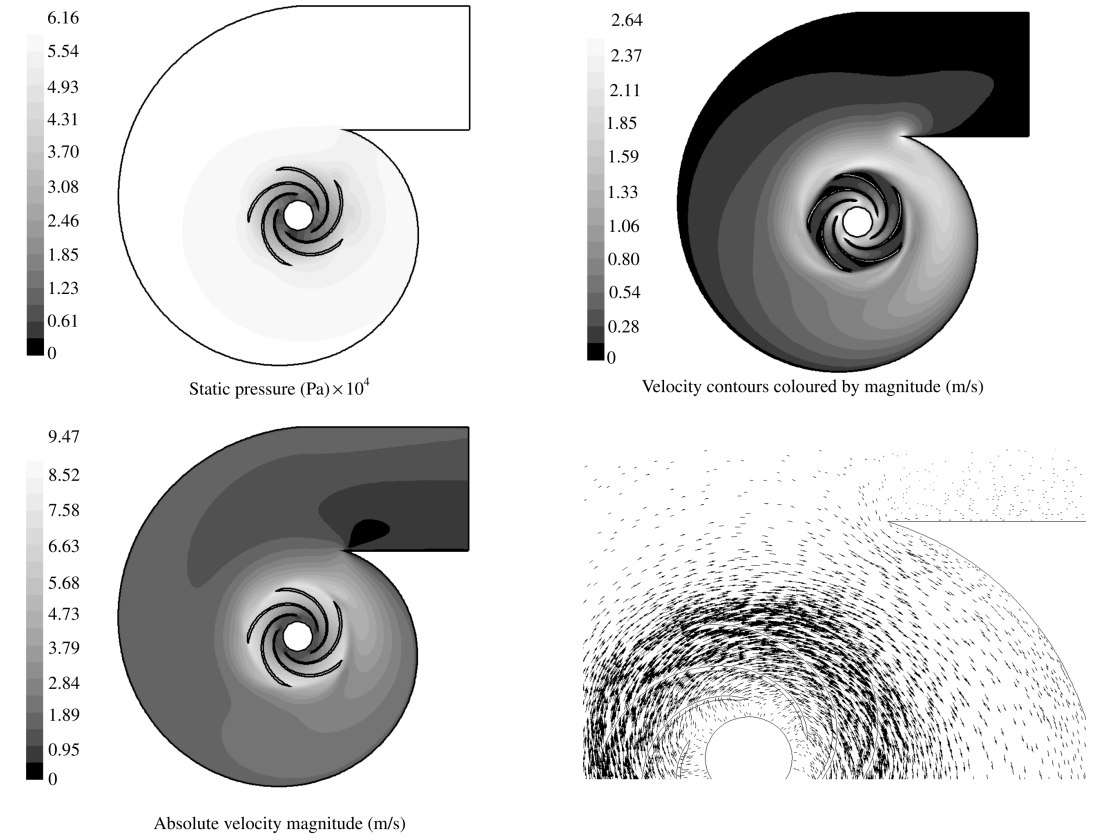


Fig. 13 Flow characteristics without the diffuser at the 1.96 l/s flowrate

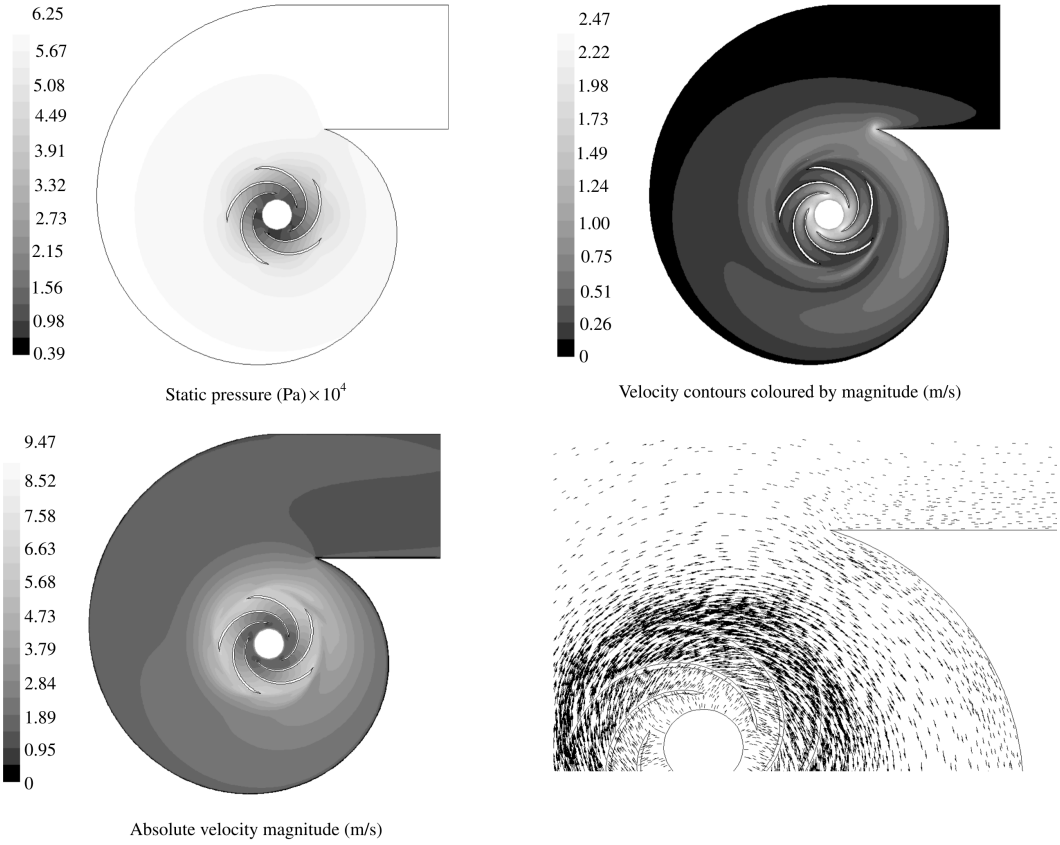


Fig. 14 Flow characteristics without the diffuser at the 2.86 l/s flowrate

5.3 Volute flows

The pump was also arranged without the diffuser in order to investigate the flow separation. This is shown in Figs 12, 13 and 14 at lower flowrate levels of 1.31, 1.96 and 2.86 l/s respectively. The effect of the diffuser blades is determined from velocity vectors, which show the flow rotating around the blades without producing positive pressure recovery. The flow also reverses from the volute to the lower part of the tongue. The jet has disappeared at all levels of mass flow, especially at low flowrate levels where the stall exists.

Peripheral pressure fluctuations are calculated at the impeller and diffuser exit sections, where the radius $R_1 = 10.87\,\text{cm}$ (107 per cent of the impeller exit radius) and $R_2 = 16.32\,\text{cm}$ (107 per cent of the diffuser exit radius). The angular origin is at the edge of the tongue and increases with clockwise orientation (Fig. 15). These results are shown in Figs 16 and 17. Data were recorded on the mid-plane of the pump corresponding to the flowrate level. The static pressure around the volute is quite uniform for flowrates in the range of the best efficiency point. However, it exhibits either a maximum for low flowrates or a minimum for high flowrates in the region of $\varphi = 330$–$30°$. These non-uniform pressure distributions are related to the acceleration (high flowrates) or deceleration (low flowrates) of the fluid

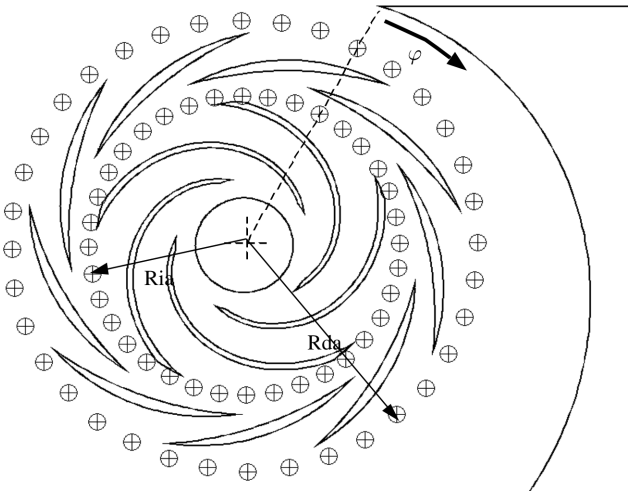


Fig. 15 The locations of the static pressure just after the impeller and diffuser

along the volute for off-design conditions. The non-uniformity of the pressure at the tongue is seen from the flow in the rotating impeller as an unsteady boundary condition; thus it affects the resulting fluctuations in the pressure field. It can be observed, for nominal and higher flowrates, that the mean difference divided by the mean value of the fluctuation is around 20 per cent (this

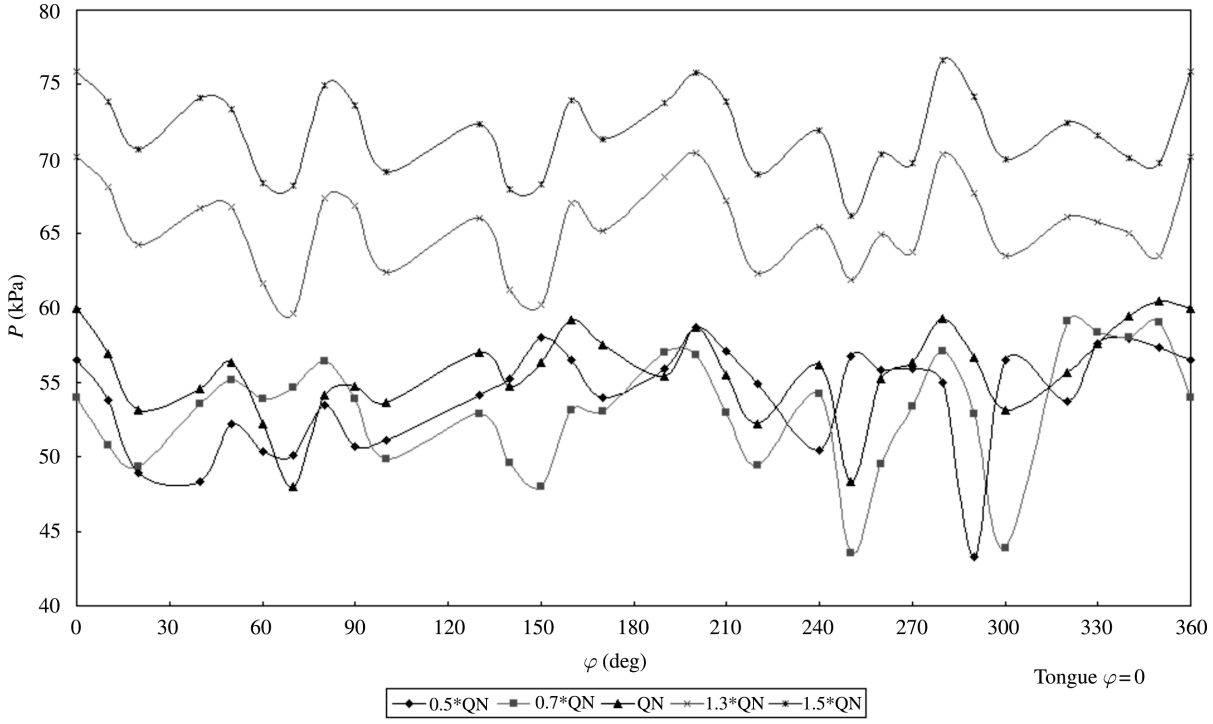


Fig. 16 The pressure fluctuations at the blade passing frequency within the impeller–diffuser vaneless space

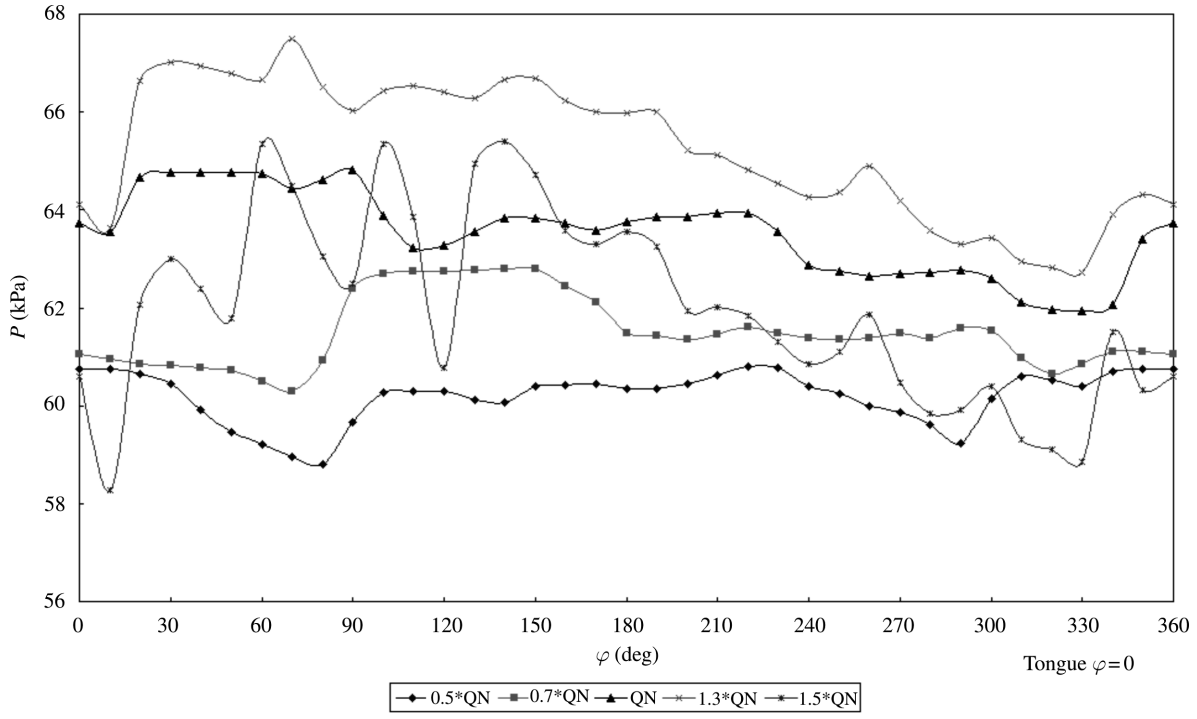


Fig. 17 The pressure fluctuations at the blade passing frequency at the exit of the diffuser

is a very good result when compared with the average static pressure, which is around 100 times higher).

The pressure fluctuations at the hub and shroud side for the impeller and diffuser exit results are observed to show no significant difference due to the small axial width (1.27 cm).

6 CONCLUSIONS

From the numerical results and discussions, the following conclusions are drawn:

1. The performance curve for the centrifugal pump,

generated using the FLUENT solver, shows a good approximation to experimental results.
2. The flow instabilities in the diffuser, such as the rotating stall and asymmetric stall, occur at lower flow levels, which is in good agreement with the observations of Sinha *et al.* [**6**].
3. Switching between the reverse and jet flows in the diffuser channel was observed under the rotating stall condition. This is mainly flow dependent.
4. The diffuser exerts a significant effect in the pump where the flow is not discharging effectively at the design point.
5. The inlet distortion of the diffuser accelerates the development and merges the boundary layers of the hub and shroud side of the diffuser walls. The axial distortion is presumed not to take the diffuser into account at a smaller axial width.
6. The pressure fluctuations around the impeller and the diffuser were found to be highly dependent on the flowrate. In particular, the amplitude of the fluctuations is greater at off-design conditions and more stable at the design flowrate.

ACKNOWLEDGEMENTS

This study was supported by the Cumhuriyet University Research Council under Grant M170. The authors wish to express their appreciation for their financial support and encouragement.

REFERENCES

1 **Emmons, H. W., Kronauer, R. E.** and **Rockett, J. A.** A survey of stall propagation—experiment and theory. *Trans ASME, J. Basic Engng*., 1959, **81**, 409–416.
2 **Yoshida, Y., Murakami, Y., Tsurusaki, T.** and **Tsujimoto, Y.** Rotating stalls in centrifugal impeller/vaned diffuser systems. In Proceedings of the First ASME/JSME Joint Fluids Engineering Conference, 1991, FED-107, pp. 125–130.
3 **Ogata, M.** and **Ichiro, A.** An experimental study of rotating stall in a radial vaned diffuser. In *Unsteady Aerodynamics and Aeroelasticity of Turbomachines*, 1995, pp. 625–641.
4 **Tsurusaki, H.** and **Kinoshita, T.** Flow control of rotating stall in a radial vaneless diffuser. *Trans. ASME*, 2001, **123**, 281–286.
5 **Parrondo, J. L., Fernandez, J., Gonzales, J.** and **Fernandez, L.** An experimental study on the unsteady pressure distribution around the impeller outlet of a centrifugal pump. In Proceedings of ASME, Boston, Massachusetts, 2000, FEDSM00–11302.
6 **Sinha, M., Pinarbasi, A.** and **Katz, J.** The flow structure during onset and development states of rotating stall within a vaned diffuser of a centrifugal pump. *Trans. ASME*, 2001, **123**, 490–499.
7 **Gonzales, J., Fernandez, J., Blanco, E.** and **Santolaria, C.** Numerical study of the dynamic effects due to impeller–volute interaction in a centrifugal pump. *Trans. ASME*, 2002, **124**, 348–355.
8 **Shi, F.** and **Tsukamoto, H.** Numerical study of pressure fluctuations caused by impeller–diffuser interaction in a diffuser pump stage. *Trans. ASME*, 2001, **123**, 466–474.
9 **Sano, T., Yoshida, Y., Tsujimoto, Y., Nakamura, Y.** and **Matsushima, T.** Numerical study of rotating stall in a pump vaned diffuser. *Trans. ASME*, 2002, **124**, 363–370.